molecular pharmaceutics

Article

pubs.acs.org/molecularpharmaceutics

Imaging Sites of Infection Using a ^{99m}Tc-Labeled Folate Conjugate Targeted to Folate Receptor Positive Macrophages

Walter A. Henne,*[,†,‡] Ryan Rothenbuhler,[†] Wilfredo Ayala-Lopez,[†] Wei Xia,[†] Bindu Varghese,[†] and Philip S. Low*[,†]

[†]Department of Chemistry, Purdue University, West Lafayette, Indiana 47907, United States

[‡]Division of Science, Governors State University, University Park, Illinois 60484, United States

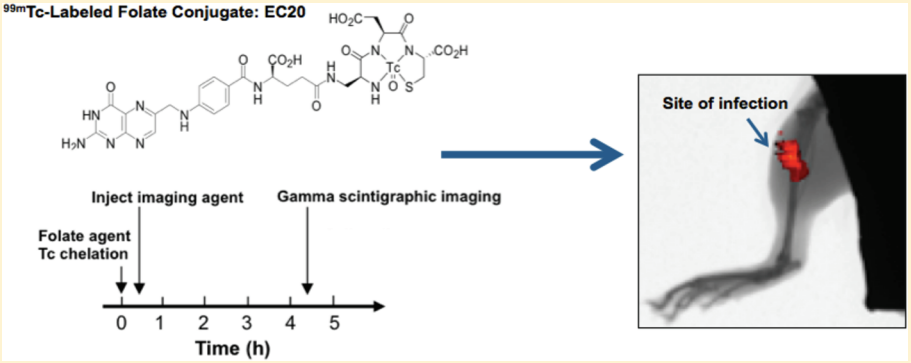

ABSTRACT: EC20, a folate-targeted ^{99m}Tc based radioimaging agent with a high folate receptor (FR) binding affinity, has been used for both the diagnosis and the staging of FR positive malignancies (currently in phase III trials) and also for the localization of inflamed lesions characterized by the accumulation of FR+ macrophages. Because recent evidence has suggested that FR+ macrophages might accumulate at sites of infectious disease, this study evaluated whether EC20 might prove similarly useful for imaging bacterial infection foci. Using gamma scintigraphic imaging, it was demonstrated that EC20 accumulated at sites of *Staphylococcus aureus* infection with a significant difference ($P < 0.0001$, $n = 12$) in enrichment noted between infected and noninfected limbs. Confirmation that the elevated uptake of EC20 in infected limbs was FR-mediated was supported by suppression of EC20 accumulation in the presence of a 200-fold excess of free folic acid ($P < 0.0001$, $n = 12$). This study establishes for the first time the use of EC20 to image and localize sites of infectious disease.

KEYWORDS: *folate, folic acid, EC20, technetium, infection imaging, macrophage, gamma scintigraphy*

INTRODUCTION

The localization of sites of infection remains a significant clinical challenge. Scintigraphic imaging using radiolabeled leukocytes[1] is the current "gold standard" for imaging infection foci; however, preparation of the labeled leukocytes is labor-intensive, may require transport of the patient's blood to distant sites, is time-consuming, and aggravates the risk of infection to both patients and health care workers.[2] Second generation methods for localizing infections have employed radiolabeled murine antibodies (Granuloscint),[3] antibody fragments (Leukoscan),[4,5] or cytokines (IL-8)[6,7] and have yielded results comparable to those with labeled leukocytes. However, costs and challenges associated with generating protein-based reagents have limited their widespread use. Alternative, nonprotein-based strategies include radiolabeled antimicrobial peptides (e.g., peptide fragments of ubiquicidin)[8,9] and antibiotics (ciprofloxacin)[10,11] among others and are currently in various stages of development. Together, these reports indicate a continuing need for improved methods for localizing and monitoring infectious disease, especially methods that can be easily performed by in primary health care facilities.

The folate receptor (FR) and its various isoforms are overexpressed on a variety of cancers (including ovarian, lung, kidney, breast, and endometrial cancers) and on activated macrophages.[12−14] Accordingly, folic acid (MW = 441.4 Da) has been exploited as a targeting ligand to deliver attached imaging and therapeutic cargos to the above pathologic loci. Cargos that have been successfully targeted with folic acid to cancers or inflamed tissues include: (i) chemotherapeutic agents,[15−17] (ii) liposomes with entrapped drugs,[18] (iii) immunotherapeutic agents,[19] and (iv) radio and optical imaging agents.[20−23] Depending on the application, the popularity of folate as a targeting ligand may be due to its ease of conjugation, specificity for pathologic tissues, stability *in vitro* and *in vivo*, facile penetration to diseased tissues, rapid internalization by FR-expressing cells, lack of immunogenicity,

Received: January 8, 2012
Revised: February 25, 2012
Accepted: March 6, 2012
Published: April 2, 2012

high affinity for a FR, and/or lack of major side effects in nontargeted organs.[13]

EC20 (Figure 1A),[23] a low molecular weight (745.2 Da) folate-conjugated ^{99m}Tc chelating agent, binds FR with a $K_d \sim 3$ nM and clears rapidly (I.V. plasma $t_{1/2} \sim 4$ min) from FR-negative tissues.[24,25] Because of its rapid clearance (images can be obtained in humans within 2 h of intravenous injection) and the absence of associated toxicity, the diagnostic agent has become attractive for imaging a diversity of pathologies.[24,25] Although a number of folate-targeted imaging modalities have been explored in preclinical studies,[20,21,26−28] only EC20 has progressed to phase III human clinical trials, where it is undergoing evaluation for the diagnosis and staging of FR+ cancers. Because of its likely continued availability in the clinic, EC20 represents a possible folate-targeted imaging agent for the development of future applications.

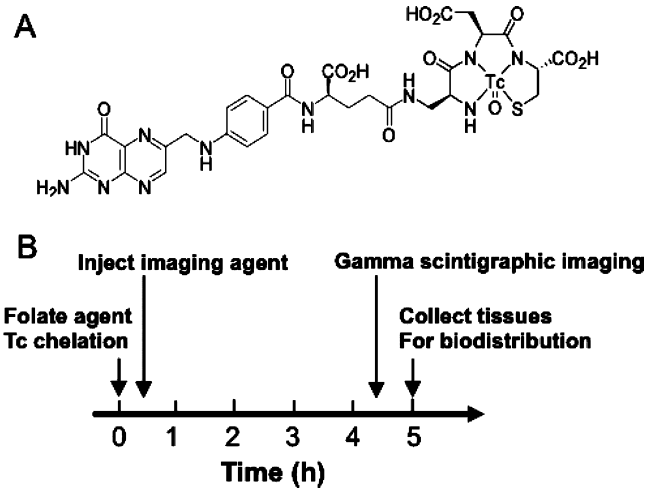

Figure 1. Structure of the folate imaging agent, EC20 (A) and experimental protocol for EC20 based imaging of bacterial infections (B).

As part of the innate immune system, macrophages recognize pathogen-associated molecular patterns (e.g., via toll-like receptors), orchestrate recruitment of other immune cells via secretion of chemokines, and so forth, and directly kill invading microbes by phagocytosis and exposure to reactive oxygen species. Our group has recently demonstrated that an activated subset of macrophages accumulates at sites of inflammation/infection and exhibits uptake of folate conjugates via a functional FR.[29] Other laboratories have similarly shown that FR+ macrophages accumulate in inflamed lesions and immunosuppressive tumor masses.[30,31] Based on the success of EC20 in imaging FR+ cancers, we decided to explore whether it might be similarly useful for imaging sites of infection. In this report, we demonstrate that EC20 can be successfully applied for the diagnosis and localization of infection foci.

EXPERIMENTAL SECTION

Materials. EC20 (a folate-linked chelator of ^{99m}Tc) was obtained from Endocyte, Inc. (West Lafayette, IN). ^{99m}Tc-labeled sodium pertechnetate was purchased from Cardinal Health Services (Indianapolis, IN). Folic acid and Sephadex G-10 beads were obtained from Sigma-Aldrich (St. Louis, MO), and tryptic soy agar (BD 236950) plus tryptic soy broth (BD 211825) were purchased from Becton Dickinson (Franklin Lakes, NJ). *Staphylococcus aureus* (ATCC No. BAA-934) was obtained from the American Type Culture Collection (ATCC, Manassas, VA). TriColor-conjugated monoclonal antibody against mouse F4/80 was purchased from CALTAG (Invitrogen), and folate Oregon Green was synthesized in-house. The 6−8 week old male Balb/C mice were obtained from Harlan Laboratories (Indianapolis, IN) and used in accordance with Purdue University animal care and use committee guidelines.

Maintenance of Bacterial Cultures. *Staphylococcus aureus* BAA-934 was propagated according to the protocol supplied by ATCC. Briefly, cultures were grown on tryptic soy agar plates or in broth at 37 °C for 24 h. For the induction of infection, bacteria were grown to an OD600 of 1.0 overnight in tryptic soy broth and used without further culturing. Proper biosafety level 2 guidelines were followed in accordance with CDC and Purdue biosafety protocols.

Animal Model of *S. aureus* Infection. Infection was induced in the caudal muscle (thigh) of Balb/C (~20 g) mice as previously described.[32] Briefly, on day one 1×10^7 CFU of *S. aureus* in 50 μL of tryptic soy broth containing 0.08 g/mL G10 Sephadex beads was injected in the posterior right caudal muscular region (thigh) of the mouse. All animals developed abscesses detectable as palpable masses within 24−48 h after inoculation. Animals were given *ad libitum* access to standard mouse chow and water throughout the course of the study as previously described.[29,33] Animals were monitored on a daily basis to assess their heath status in accordance with Purdue animal care and safety guidelines.

Flow Cytometric Analysis of FR+ Macrophages in Infected Mice. *S. aureus*-recruited macrophages were isolated via peritoneal lavage (8 mL of phosphate-buffered saline, PBS) 4 days after intraperitoneal (ip) injection of 1×10^6 CFU live *S. aureus*. Cells were washed with PBS twice and resuspended in folate-deficient Roswell Park Memorial Institute medium (RPMI). Cell suspensions were incubated with the appropriate antibodies for 30 min on ice. Samples were washed three times in PBS followed by incubation with folate-Oregon Green conjugate (100 nM) for 30 min at 37 °C. In some cases, cells were coincubated with 100 μM folic acid to competitively block all FR. In all experiments, appropriate isotype controls were used. Flow cytometry was performed on a BD FACSCalibur flow cytometer equipped with CELLQUEST software (Becton Dickinson, San Jose, CA) for acquisition and analysis, as previously described.[29]

Standard Scintigraphic Imaging of Mice and Biodistribution Analysis with EC20. Complexation of EC20 with ^{99m}Tc was performed as previously described.[23,29] Mice were injected ip four days post-infection with 37 MBq (~400 nmol/kg) EC20 or 37 MBq EC20 plus a 200-fold molar excess of folic acid (~80 μM/kg adjusted to pH = 7.4). For imaging purposes, 4 h after injection mice were positioned in ventral recumbency and imaged using a Medical Imaging Electronics gamma scintigraphy instrument (Elk Grove Village, Il) equipped with ProcessX imaging software for region of interest (ROI) analysis (Figure 1B). Image acquisition was performed for 5 min, and gamma emission from the abdomen and thorax was shielded using 1/8 in. lead plates. For biodistribution studies, mice were then sacrificed and their respective tissues harvested, weighed, and analyzed using a gamma counter (Packard BioScience, Meridin, CT). Results were expressed as the percentage injected dose per gram of tissue (%ID/g).

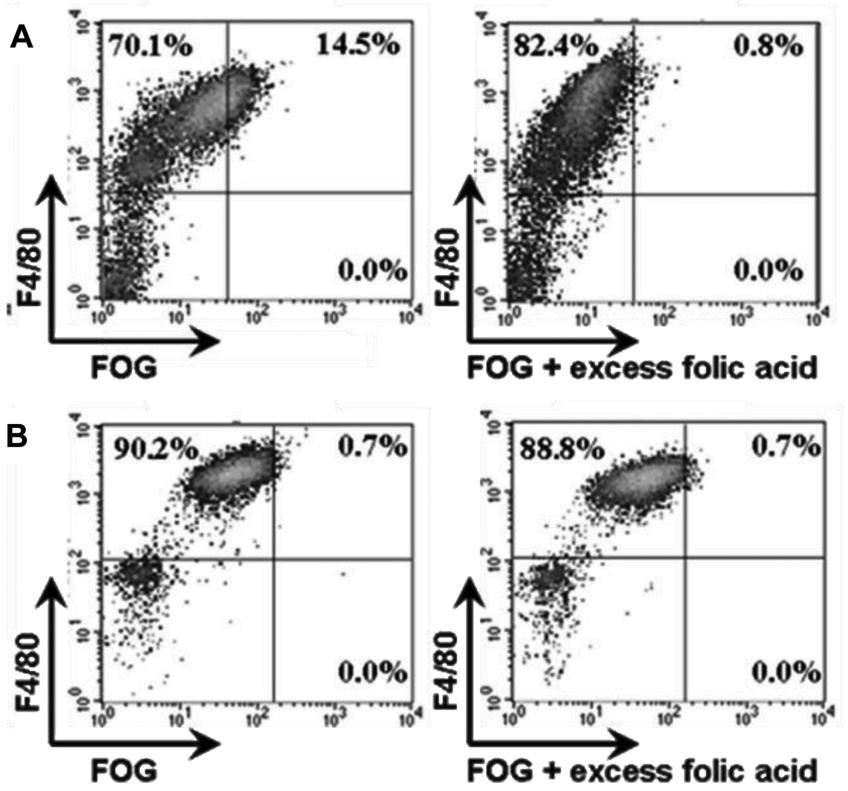

Figure 2. Expression of FRs on F4/80$^+$ macrophages recruited by *S. aureus*. Cells isolated from the peritoneal cavity of mice injected 4 days prior with either *S. aureus* (A) or sterile saline (B) were analyzed by flow cytometry for the binding of anti-F4/80 antibody and folate-Oregon Green. To demonstrate that folate-Oregon Green (FOG) binding is mediated exclusively by FR, the same cell isolates were coincubated with 1000-fold molar excess of folic acid and examined by flow cytometry (right panels). The percentage of macrophages costained with the F4/80 macrophage marker and FOG are indicated in each respective quadrant.

Spatially Co-registered Radioisotopic, Radiographic, and Reflectance Imaging. Preparation of the mice for imaging was performed as described above, except images were obtained on a Kodak In Vivo FX imaging station. Spatially coregistered images, image acquisition, optimization, and overlays were performed using Kodak Molecular Imaging Software v. 4.5.1. All images had a focus setting of 7 mm to match the distance of the animal imaging chamber above the platen, and the field of view was set to 20 × 20 cm (100 μm/pixel). For reflectance mode images, data were acquired for 0.05 s using a white illumination source, no emission filter, and an *f*-stop ring setting of 11. Radioisotopic images were acquired for 20 s using a Kodak radioisotopic phosphor screen (Catalog No. 8527715) with no illumination source, binning set to 4 × 4, and an *f*-stop ring setting of 0. Radiographic images were acquired for 240 s using a Kodak radiographic phosphor screen (Catalog No. 8509051) with no light source. X-ray images were acquired with the following settings: energy of 35 KVP, current of 149 μA, 0.5 mm X-ray filter, and an *f*-stop ring setting of 4. These settings represent minor modifications of standard methods recommended by the manufacturer.

Statistical Methods. The statistical significance between groups was assessed using the Student's *t*-test. *P* values less than 0.05 were considered significant.

RESULTS

Evaluation of FR+ Macrophages Isolated from *S. aureus* Infected Mice. To establish whether infection with *S. aureus* might promote accumulation of FR-expressing macrophages, mice were injected ip with *S. aureus* (SA), and peritoneal cells were harvested by lavage 4 days later. After incubation with folate-Oregon Green and a macrophage-specific antibody (anti-F4/80), cells were analyzed by flow cytometry for FR expression on F4/80+ macrophages. As seen in Figure 2A (left panel), a subpopulation of peritoneal macrophages (F4/80+ cells) from infected mice bound high levels of folate-Oregon Green. Moreover, uptake of the folate-Oregon Green was quantitatively inhibited by a 1000-fold excess of free folic acid (Figure 2A, right panel), suggesting that binding of the targeted dye was FR mediated. More importantly, as noted in Figure 2B, folate-Oregon Green uptake was absent in control mice injected with saline, suggesting that expression of FR does not occur in resting macrophages (in agreement with Xia et al.)[29] but rather constitutes a characteristic of pathogen-stimulated macrophages.

EC20 Gamma Scintigraphic Imaging of Bacterial Infections in Mice. The ability of folate to target attached imaging agents to sites of infection *in vivo* was then examined by ip injection of the folate-^{99m}Tc imaging probe, EC20, into balb/c mice that had been previously injected in the thigh with 10^7 CFU *S. aureus*. As seen in Figure 3A, uptake of the radionuclide was primarily confined to the region in the thigh that was inoculated with bacteria. Moreover, control mice infected in the same manner but simultaneously treated with a 200-fold excess of free folic acid (competed control group) to block empty FRs displayed significantly reduced uptake, suggesting that accumulation of EC20 in the diseased lesion was FR-mediated (Figure 3B). For statistical purposes, a total

dx.doi.org/10.1021/mp3000138 | *Mol. Pharmaceutics* 2012, 9, 1435−1440

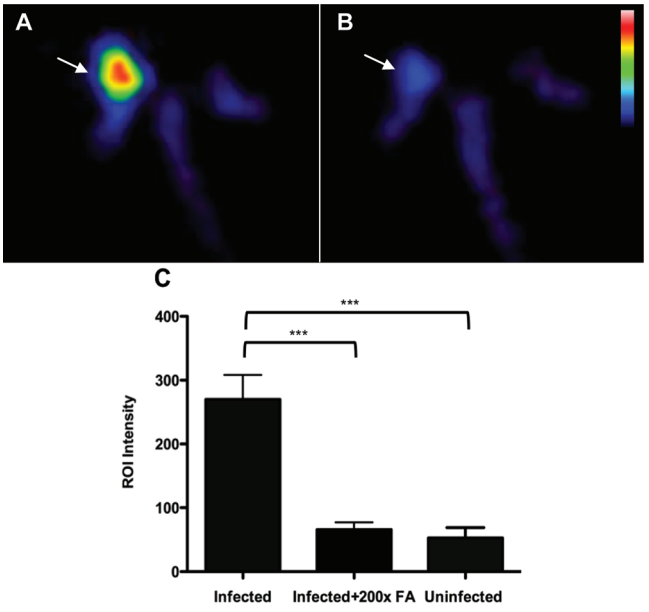

Figure 3. Representative standard gamma scintigraphic images demonstrating EC20 uptake in mice infected with *S. aureas*. Mice were infected with 10^7 CFU of *S. aureus* (indicated by arrows) in the thigh region of the right leg. Four days later, mice were dosed IP with 37 MBq EC20 (A) or 37MBq EC20 with a 200-fold excess of free folic acid (B) and imaged in the ventral recumbancy position 4 h later. Competition (B) confirmed folate-mediated uptake of EC20. (C) Based on region of interest comparisons (ROI), significant differences were noted between the infected limb versus the infected limb with a competing dose of folic acid (***$P < 0.0001$, $n = 12$) and between infected and uninfected limbs on the same animal (***$P < 0.0001$, $n = 12$), respectively. Note: the kidney and bladder were shielded with an 1/8 in. lead plate to better visualize the foci.

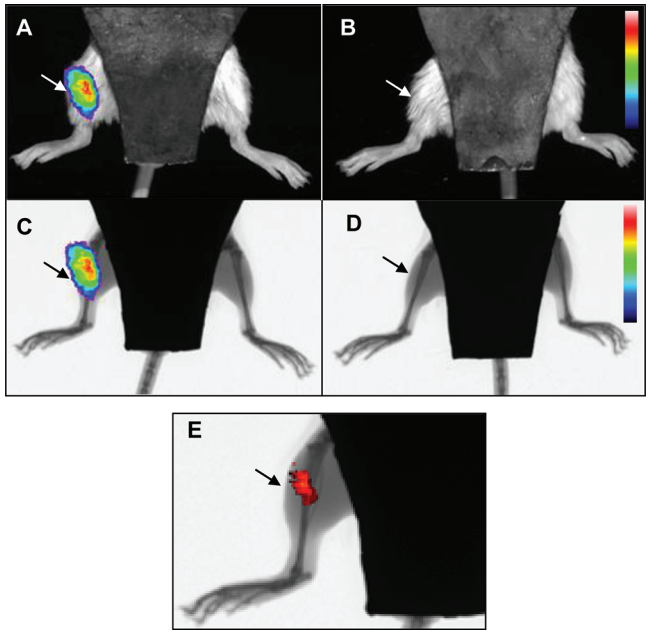

Figure 4. Representative radioisotopic images demonstrating EC20 uptake in mice infected with *S. aureus* (site of injection indicated by arrows) coregistered with both reflective and radiographic images using a Kodak imaging workstation. Mice were infected with 10^7 CFU *S. aureus* and dosed IP with 37 MBq EC20 identically as described for standard gamma scintigraphy (A and C: coregistered reflective image) or 37 MBq EC20 with a 200-fold excess of free folic acid (B and D: coregistered radiographic image) and imaged in the ventral recumbancy position 4 h later. Using the imaging software, the saturation was adjusted to define the area of highest radio-isotopic uptake (E), which enabled enhanced visualization of the infection foci. As with standard gamma scintigraphy, the kidney and bladder were shielded with an 1/8 in. lead plate to better visualize the foci.

of 12 pairs of mice (±competition with free folate) were imaged using the same protocol, and ROI counts were determined. As anticipated, a significant difference (269.6 ± 11.7 for infected vs 52.7 + 4.9 for infected plus competition; $P < 0.0001$, $n = 12$) between groups was noted (Figure 3C). Further, when infected right limbs (269.6 ± 11.7) were compared with noninfected left limbs (65.7 ± 3.5) in the same mice, a similar significant difference was observed (Figure 3C, $P < 0.0001$, $n = 12$). For accuracy of ROI analyses, radioactivity from the kidneys and bladder was blocked with a 1/8 in. thick lead shield.

Spatially Co-registered Radioisotopic, Radiographic, and Reflectance Images. To more accurately localize the bacterial infection in the anatomy of the infected animals, white light, X-ray, and radioisotopic images of the same mice were obtained and aligned using a Kodak imaging workstation and associated software. Figure 4 (panel A and B) shows the reflectance (white light) image coregistered with the corresponding radioisotope image, and panels C and D show the same radioisotope image coregistered with the appropriate radiographic (X-ray) image. As noted in the figure, uptake was limited to the infected thigh region, consistent with the standard gamma scintigraphic images shown previously. More importantly, when the image intensity was adjusted to reveal only the most intense regions of radioactivity, the site of EC20 accumulation was invariably found to coincide with the site of pathogen injection, based on anatomical landmarks (Figure 4E).

Biodistribution of EC20 in Infected Mice. Biodistribution analysis (Figure 5A,B) confirmed that the major sites of EC20 accumulation were limited to the kidneys, liver, and infected right limbs (8.97% ID/g, 1.38% ID/g, and 0.53% ID/g, respectively) of the animals. Uptake in the kidneys is well-established to stem from FR expression on the apical surface of the proximal tubules, where folates filtered into the urine are transcytosed across the kidney epithelium back into the bloodstream.[34] Uptake in the liver is thought to derive from resident macrophages that become activated in response to toll-like receptor ligands released by bacteria, fat cells, or some other endogenous source. Accumulation of the folate probe in the infected leg is consistent with accumulation of FR+ activated macrophages at other sites of bacterial infection.

Due to the inherent difficulty in distinguishing infected from noninfected tissue by visual inspection, no effort was made to excise and count only infected foci. Instead, the whole leg was resected, weighed, and counted from each mouse for biodistribution analysis. As a consequence, the % ID/g leg tissue primarily contains counts from noninfected muscle and bone, with only a small contribution from the actual sites of infection. Despite this dilution effect, a significant difference (Figure 5B, $P < 0.05$, $n = 4$) was noted between the right (infected) limbs and competed control limbs (mice administered EC20 plus a 200-fold excess acid) and between the infected and the noninfected limbs of the same animal (Figure 5B, $P < 0.05$, $n = 4$).

dx.doi.org/10.1021/mp3000138 | *Mol. Pharmaceutics* 2012, 9, 1435–1440

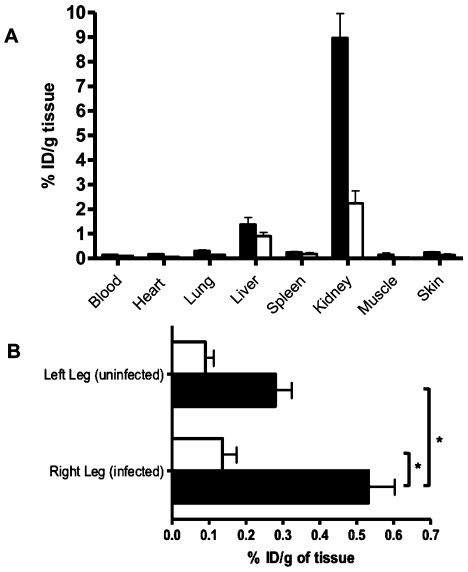

Figure 5. Biodistribution (A and B) of EC20 in infected mice. Mice were injected ip with 37 MBq of the folate imaging agent, EC20, and sacrificed 4 h later. Tissues were harvested, and the uptake of the EC20 determined by gamma counting (expressed as percent injected dose per gram tissue). Graph B represents uptake of the radio-tracer in both the infected and noninfected limbs (highest uptake: kidney = 8.97, liver = 1.38, infected limb = 0.53). Black bars and white bars indicate infected mice and infected mice predosed with a 200-fold excess of folic acid, respectively (n = 4 per group, mean ± SEM). *P < 0.05.

■ DISCUSSION

Use of *ex vivo* labeled autologous leukocytes has proven effective in clinical settings for the diagnosis and localization of infectious disease associated with such conditions as septic arthritis, diverticulitits, endocarditis, osteomyelitis, and post-surgical infections.[35,36] The delineation of the site and extent of infection have been found to reduce morbidity and mortality, limit hospitalization costs, and aid in the guidance of biopsy procedures.[3,37] Although labeled leukocyte imaging remains the clinical "gold standard" for detecting hidden infections, improved methods based on a diversity of mechanisms are currently being sought. In this report, we have demonstrated that a folate-targeted ^{99m}Tc radiotracer, EC20, can yield excellent images of *S. aureus* infection sites. Because of its ease of synthesis, high radiolabeling efficiency, rapid accumulation in infected areas, lack of systemic toxicity, and desirable pharmacokinetics (good imaging contrast is achieved in 4 h compared to days for whole cell or antibody based imaging agents),[23−25] EC20 warrants further examination as a possible substitute for the more cumbersome current protocols. Thus, except when the localized infection occurs in the liver, where nonspecific uptake of EC20 is often observed, good contrast should be seen between the diseased tissue and surrounding healthy tissue, especially if a high resolution imaging modality such as single-photon emission computed tomography (SPECT) is employed.

In agreement with the imaging experiments, biodistribution data revealed greater uptake of the radiotracer in the infected limb than the competed control limb (0.53 ± 0.14% ID/g vs 0.13 ± 0.04% ID/g); however, a modest increase in uptake was also unexpectedly observed in the opposite (noninfected) limb of each infected animal (0.28 ± 0.09% ID/g). We hypothesize that this elevated uptake may derive from a mild systemic inflammation associated with the localized infection. Thus, although no indications of systemic illness were ever noted in the infected mice and no focal infections were visualized in uninfected limbs, it is conceivable that a systemic increase in inflammatory cytokines could have enhanced the activation state of macrophages even in uninfected limbs. Consistent with this interpretation, Turk et al. have previously reported a systemic inflammatory response in rats treated to develop a localized form of experimental autoimmune (rheumatoid) arthritis.[38] In this latter study, increased levels of EC20 uptake were also observed in the internal organs (e.g., lung, liver, spleen) of the arthritic animals, and this uptake could be blocked by excess folic acid.

■ CONCLUSIONS

This report demonstrates the use of the folate radiotracer, EC20, for infection imaging based upon its selective uptake in FR+ activated macrophages that accumulate at sites of infection. To our knowledge, this study is the first demonstration of folate-based agents used for this purpose. Given recent evidence that FR is expressed on activated macrophages during infection with several bacterial strains including *S. aureus* outlined in this report, it is anticipated that this imaging strategy can be extended to other types of infection. Further studies involving different bacterial strains and imaging modalities are in progress to assess the full capability of this imaging agent for detection and localization of infectious disease.

■ AUTHOR INFORMATION

Corresponding Author

*Mailing address: Philip S. Low, Ph.D., Ralph C. Corley Distinguished Professor of Chemistry, Department of Chemistry, Purdue University, 560 Oval Drive, West Lafayette, IN 47907. Phone: (765) 494-5273. Fax: (765) 494-5272. E-mail: plow@purdue.edu. Mailing address: Walter A. Henne, Ph.D., Assistant Professor of Chemistry, Division of Science, Governors State University, 1 University Parkway, University Park, IL 60484. Phone: (708) 235-7395; (765) 714-5698 (cell). Fax: (708) 534-1641. E-mail: whenne@govst.edu.

Notes

The authors declare the following competing financial interest(s):P.S.L. has received fees and stock from Endocyte, Inc. (West Lafayette, IN, USA), a company that he founded in 1995 to develop treatments for cancer and inflammation. W.A.H. owns stock in Endocyte, Inc. Purdue University has applied for a patent claiming this infection imaging method as intellectual property. The authors declare that they have no other competing interests.

■ ACKNOWLEDGMENTS

We wish to thank Derek Doorneweerd, Andrew Hilgenbrink, Erina Vlashi, and Kristene Henne for their valuable assistance.

■ REFERENCES

(1) Thakur, M. L.; Lavender, J. P.; Arnot, R. N.; Silvester, D. J.; Segal, A. W. Indium-111-labeled autologous leukocytes in man. *J. Nucl. Med.* **1977**, *18* (10), 1014−21.

(2) Palestro, C. J. In vivo leukocyte labeling: the quest continues. *J. Nucl. Med.* **2007**, *48* (3), 332−4.

(3) Weiner, R. E.; Thakur, M. L. Imaging infection/inflammations. Pathophysiologic basis and radiopharmaceuticals. *Q. J. Nucl. Med.* **1999**, *43* (1), 2−8.

(4) Becker, W.; Bair, J.; Behr, T.; Repp, R.; Streckenbach, H.; Beck, H.; Gramatzki, M.; Winship, M. J.; Goldenberg, D. M.; Wolf, F. Detection of soft-tissue infections and osteomyelitis using a technetium-99m-labeled anti-granulocyte monoclonal antibody fragment. *J. Nucl. Med.* **1994**, *35* (9), 1436−43.
(5) Becker, W.; Palestro, C. J.; Winship, J.; Feld, T.; Pinsky, C. M.; Wolf, F.; Goldenberg, D. M. Rapid imaging of infections with a monoclonal antibody fragment (LeukoScan). *Clin. Orthop. Relat. Res.* **1996**, *329*, 263−72.
(6) Rennen, H. J.; Boerman, O. C.; Oyen, W. J.; van der Meer, J. W.; Corstens, F. H. Specific and rapid scintigraphic detection of infection with 99mTc-labeled interleukin-8. *J. Nucl. Med.* **2001**, *42* (1), 117−23.
(7) Bleeker-Rovers, C. P.; Rennen, H. J.; Boerman, O. C.; Wymenga, A. B.; Visser, E. P.; Bakker, J. H.; van der Meer, J. W.; Corstens, F. H.; Oyen, W. J. 99mTc-labeled interleukin 8 for the scintigraphic detection of infection and inflammation: first clinical evaluation. *J. Nucl. Med.* **2007**, *48* (3), 337−43.
(8) Akhtar, M. S.; Qaisar, A.; Irfanullah, J.; Iqbal, J.; Khan, B.; Jehangir, M.; Nadeem, M. A.; Khan, M. A.; Afzal, M. S.; Ul-Haq, I.; Imran, M. B. Antimicrobial peptide 99mTc-ubiquicidin 29−41 as human infection-imaging agent: clinical trial. *J. Nucl. Med.* **2005**, *46* (4), 567−73.
(9) Welling, M. M.; Paulusma-Annema, A.; Balter, H. S.; Pauwels, E. K.; Nibbering, P. H. Technetium-99m labelled antimicrobial peptides discriminate between bacterial infections and sterile inflammations. *Eur. J. Nucl. Med.* **2000**, *27* (3), 292−301.
(10) Vinjamuri, S.; Hall, A. V.; Solanki, K. K.; Bomanji, J.; Siraj, Q.; O'Shaughnessy, E.; Das, S. S.; Britton, K. E. Comparison of 99mTc infecton imaging with radiolabelled white-cell imaging in the evaluation of bacterial infection. *Lancet* **1996**, *347* (8996), 233−5.
(11) Britton, K. E.; Vinjamuri, S.; Hall, A. V.; Solanki, K.; Siraj, Q. H.; Bomanji, J.; Das, S. Clinical evaluation of technetium-99m infecton for the localisation of bacterial infection. *Eur. J. Nucl. Med.* **1997**, *24* (5), 553−6.
(12) Ross, J. F.; Chaudhuri, P. K.; Ratnam, M. Differential regulation of folate receptor isoforms in normal and malignant tissues in vivo and in established cell lines. Physiologic and clinical implications. *Cancer* **1994**, *73* (9), 2432−43.
(13) Low, P. S.; Henne, W. A.; Doorneweerd, D. D. Discovery and development of folic-acid-based receptor targeting for imaging and therapy of cancer and inflammatory diseases. *Acc. Chem. Res.* **2008**, *41* (1), 120−9.
(14) Nakashima-Matsushita, N.; Homma, T.; Yu, S.; Matsuda, T.; Sunahara, N.; Nakamura, T.; Tsukano, M.; Ratnam, M.; Matsuyama, T. Selective expression of folate receptor beta and its possible role in methotrexate transport in synovial macrophages from patients with rheumatoid arthritis. *Arthritis Rheum.* **1999**, *42* (8), 1609−16.
(15) Henne, W. A.; Doorneweerd, D. D.; Hilgenbrink, A. R.; Kularatne, S. A.; Low, P. S. Synthesis and activity of a folate peptide camptothecin prodrug. *Bioorg. Med. Chem. Lett.* **2006**, *16* (20), 5350−5.
(16) Leamon, C. P.; Reddy, J. A. Folate-targeted chemotherapy. *Adv. Drug Delivery Rev.* **2004**, *56* (8), 1127−41.
(17) Leamon, C. P.; Reddy, J. A.; Vlahov, I. R.; Vetzel, M.; Parker, N.; Nicoson, J. S.; Xu, L. C.; Westrick, E. Synthesis and biological evaluation of EC72: a new folate-targeted chemotherapeutic. *Bioconjug Chem* **2005**, *16* (4), 803−11.
(18) Lee, R. J.; Low, P. S. Delivery of liposomes into cultured KB cells via folate receptor-mediated endocytosis. *J. Biol. Chem.* **1994**, *269*, 3198−3204.
(19) Yi, Y. S.; Ayala-Lopez, W.; Kularatne, S. A.; Low, P. S. Folate-targeted hapten immunotherapy of adjuvant-induced arthritis: comparison of hapten potencies. *Mol. Pharmaceutics* **2009**, *6* (4), 1228−36.
(20) Mathias, C. J.; Hubers, D.; Low, P. S.; Green, M. A. Synthesis of [(99m)Tc]DTPA-folate and its evaluation as a folate-receptor-targeted radiopharmaceutical. *Bioconjugate Chem.* **2000**, *11* (2), 253−7.
(21) Mathias, C. J.; Wang, S.; Low, P. S.; Waters, D. J.; Green, M. A. Receptor-mediated targeting of 67Ga-deferoxamine-folate to folate-receptor-positive human KB tumor xenografts. *Nucl. Med. Biol.* **1999**, *26* (1), 23−5.
(22) Kennedy, M. D.; Jallad, K. N.; Thompson, D. H.; Ben-Amotz, D.; Low, P. S. Optical imaging of metastatic tumors using a folate-targeted fluorescent probe. *J. Biomed. Opt.* **2003**, *8* (4), 636−41.
(23) Leamon, C. P.; Parker, M. A.; Vlahov, I. R.; Xu, L. C.; Reddy, J. A.; Vetzel, M.; Douglas, N. Synthesis and biological evaluation of EC20: a new folate-derived, (99m)Tc-based radiopharmaceutical. *Bioconjugate Chem.* **2002**, *13* (6), 1200−10.
(24) Fisher, R. E.; Siegel, B. A.; Edell, S. L.; Oyesiku, N. M.; Morgenstern, D. E.; Messmann, R. A.; Amato, R. J. Exploratory study of 99mTc-EC20 imaging for identifying patients with folate receptor-positive solid tumors. *J. Nucl. Med.* **2008**, *49* (6), 899−906.
(25) Reddy, J. A.; Xu, L. C.; Parker, N.; Vetzel, M.; Leamon, C. P. Preclinical evaluation of (99m)Tc-EC20 for imaging folate receptor-positive tumors. *J. Nucl. Med.* **2004**, *45* (5), 857−66.
(26) Guo, W.; Hinkle, G. H.; Lee, R. J. 99mTc-HYNIC-folate: a novel receptor-based targeted radiopharmaceutical for tumor imaging. *J. Nucl. Med.* **1999**, *40* (9), 1563−9.
(27) Ilgan, S.; Yang, D. J.; Higuchi, T.; Zareneyrizi, F.; Bayhan, H.; Yu, D.; Kim, E. E.; Podoloff, D. A. 99mTc-ethylenedicysteine-folate: a new tumor imaging agent. Synthesis, labeling and evaluation in animals. *Cancer Biother. Radiopharm.* **1998**, *13* (6), 427−35.
(28) Muller, C.; Hohn, A.; Schubiger, P. A.; Schibli, R. Preclinical evaluation of novel organometallic 99mTc-folate and 99mTc-pteroate radiotracers for folate receptor-positive tumour targeting. *Eur. J. Nucl. Med. Mol. Imaging* **2006**, *33* (9), 1007−16.
(29) Xia, W.; Hilgenbrink, A. R.; Matteson, E. L.; Lockwood, M. B.; Cheng, J. X.; Low, P. S. A functional folate receptor is induced during macrophage activation and can be used to target drugs to activated macrophages. *Blood* **2009**, *113* (2), 438−46.
(30) Puig-Kroger, A.; Sierra-Filardi, E.; Dominguez-Soto, A.; Samaniego, R.; Corcuera, M. T.; Gomez-Aguado, F.; Ratnam, M.; Sanchez-Mateos, P.; Corbi, A. L. Folate receptor beta is expressed by tumor-associated macrophages and constitutes a marker for M2 anti-inflammatory/regulatory macrophages. *Cancer Res.* **2009**, *69* (24), 9395−403.
(31) Tsuneyoshi, Y.; Tanaka, M.; Nagai, T.; Sunahara, N.; Matsuda, T.; Sonoda, T.; Ijiri, K.; Komiya, S.; Matsuyama, T. Functional folate receptor beta-expressing macrophages in osteoarthritis synovium and their M1/M2 expression profiles. *Scand. J. Rheumatol.* **2012**, DOI: 10.3109/03009742.2011.605391.
(32) Ford, C. W.; Hamel, J. C.; Stapert, D.; Yancey, R. J. Establishment of an experimental model of a Staphylococcus aureus abscess in mice by use of dextran and gelatin microcarriers. *J. Med. Microbiol.* **1989**, *28* (4), 259−66.
(33) Ayala-Lopez, W.; Xia, W.; Varghese, B.; Low, P. S. Imaging of atherosclerosis in apoliprotein e knockout mice: targeting of a folate-conjugated radiopharmaceutical to activated macrophages. *J. Nucl. Med.* **2010**, *51* (5), 768−74.
(34) Sandoval, R. M.; Kennedy, M. D.; Low, P. S.; Molitoris, B. A. Uptake and trafficking of fluorescent conjugates of folic acid in intact kidney determined using intravital two-photon microscopy. *Am. J. Physiol. Cell Physiol.* **2004**, *287* (2), C517−26.
(35) Palestro, C. J. Radionuclide imaging of infection: in search of the grail. *J. Nucl. Med.* **2009**, *50* (5), 671−3.
(36) Love, C.; Palestro, C. J. Radionuclide imaging of infection. *J. Nucl. Med. Technol.* **2004**, *32* (2), 47−57 quiz 58−9..
(37) Palestro, C. J.; Torres, M. A. Radionuclide imaging of nonosseous infection. *Q. J. Nucl. Med.* **1999**, *43* (1), 46−60.
(38) Turk, M. J.; Breur, G. J.; Widmer, W. R.; Paulos, C. M.; Xu, L. C.; Grote, L. A.; Low, P. S. Folate-targeted imaging of activated macrophages in rats with adjuvant-induced arthritis. *Arthritis Rheum.* **2002**, *46* (7), 1947−55.